Viability of unidirectional radial turbines for twin-turbine configuration of OWC wave energy converters

Laudino Rodríguez[a], Bruno Pereiras[b*], Jesús Fernández-Oro[b] and Francisco Castro[c]

[a] Centro Integrado de F.P. Mantenimiento y Servicios a la Producción de Langreo (C.I.F.P.M.S.P.)

Ciudad Tecnológica e Industrial Valnalón, Hornos Altos S/N, 33930, La Felguera, Spain

laudelinrg@gmail.com

[b] Department of Energy, University of Oviedo

Energy Building (EDZE), Campus de Viesques s/n, 33271, Gijón, Spain

* pereirasbruno@uniovi.es; jesusfo@uniovi.es

[c] Department of Energetic and Fluidmechanics Engineering. University of Valladolid

Paseo del Cauce 59, 47011, Valladolid, Spain

castro@eii.uva.es

ABSTRACT

Oscillating Water Column devices are the most widespread among Wave Energy converters, with an efficiency that is closely related to the performance of its Power Take-Off element, usually a turbine. Using unidirectional turbines requires a system of valves to rectify the bidirectional flow, so self-rectifying turbines are more convenient for an OWC device. Another recent proposal is the use of a twin turbine configuration, where an arrangement of two unidirectional turbines could perform this task, with each turbine extracting the flow energy alternately. To date, all the twin turbine configurations studied in the open literature consider unidirectional axial turbines. In this paper, the use of a radial turbine to improve the system´s efficiency by enhancing flow rectification is presented for the first time. An experimentally validated numerical model has been used to analyse the flow field of the radial turbine when working in both direct and reverse modes. Interesting conclusions are extracted. Finally, a performance comparison of the twin turbine configuration using axial or radial turbines has been carried out. It is concluded that the good performance of the radial turbine working as a flow preventer makes this kind of turbine an interesting option for twin systems.

KEY WORDS: twin turbines, OWC, wave energy, radial turbine

NOMENCLATURE

A_R	*Characteristic area*
$C_H = \Delta P / (\rho \omega^2 \; D^2)$	*Input coefficient*
$C_P = \; T_o \omega / (\rho \omega^3 \;\; D^5)$	*Power coefficient*
D	*Mean turbine diameter, =2·r_R*
Q, q	*Flow rate*
Q_{max}	*Amplitude of flow rate in unsteady conditions*
ΔP	Pressure drop (total-static)
r_R	*Blade mid-chord radius*
T_o	*Output mechanical torque*
T	*Period*
$u_R = \omega \; r_R$	*Blade velocity at r_R*
u, v, w	*Velocity components (peripheric, absolute and relative)*
α, β	*Absolute and relative flow angle*
$\eta = T_o \; \omega / \; \Delta P \; Q$	*Steady efficiency*
η_{vol}	*Volumetric efficiency*
$\bar{\eta}_{input}$	*Input mean efficiency*
$\bar{\eta}_{tg}$	*Mean efficiency of twin turbines set*
P	*Air density*
$\phi = v_R / u_R$	*Flow coefficient*
Φ	*Flow coefficient in unsteady conditions*
Ω	*Rotational speed*
Subscripts/superscripts	
1,2	*Turbine 1 or 2*
C, D	*Inner and outer rotor sections*
Direct/reverse	*Flow direction*
Total	*Sum of turbine 1 and turbine 2*

1. INTRODUCTION

Great efforts are being made within the wave energy field worldwide. Many researchers have the potential of this kind of renewable energy in their sights, so the presentation of new devices, or improvements to old ones, often appear in technical literature.

One of the most promising wave energy concepts is the so-called Oscillating Water Column (OWC), see Figure 1 top. It was one of the first solutions to be developed (Falcão, 2010) and it has currently achieved a significant level of maturity, with several projects even reaching a commercial scale (Falcão, 2010; Torre-Enciso et al., 2009). This kind of device can be placed on the shoreline, near the shore and even offshore, although most prototypes are placed onshore because this makes their installation and maintenance easier. An interesting review about OWC performance from an historical perspective and a complete list of references can be found in (Falcão and Henriques, 2016),

Essentially, OWC power plants are based on a simple working principle: a concrete or steel structure is semi-submerged in the sea and opened at the bottom, so the water-free surface is displaced as a piston inside the structure according to the wave period. As a consequence, the air contained in the top of the structure is compressed/decompressed and pushed outwards/aspirated inwards, generating a bidirectional air flow which is used to drive a Power Take-Off (PTO). The energy conversion from wave to pneumatic is made by the structure and the pneumatic energy is then turned into mechanical energy by means of a PTO element, typically a turbine

To take full advantage of the characteristics of the two-way flow generated by the OWC, the PTO element should have some special features. In the early years, a valve rectification system was used to drive a unidirectional axial turbine (Maeda et al., 2001; Setoguchi and Takao, 2006). However, the valve system would lead to maintenance and operational problems. Two alternatives were suggested to avoid the use of valves:

Self-rectifying turbines have been the most popular solution for the PTO element in OWC converters over the last decades. There are several types of these turbines and most of them can be classified in two categories: Wells turbines (Raghunathan, 1995; Wells, 1980) and impulse turbines, which can be radial (Pereiras et al., 2011b; Setoguchi et al., 2002) or axial (Babintsev, 1975; Maeda et al., 1999). Whatever the case, self-rectifying turbines have relatively poor efficiency, except those equipped with adjustable blades/guide-vanes (Curran, R.; Denniss, Tom; Boake, 2000; Falcão and Gato, 2012; Setoguchi and Takao, 2006). Unfortunately, the use of turbines with moving elements would possibly lead to additional problems in the maintenance of these facilities. More information about air turbines for OWC systems can be found in (Falcão and Gato, 2012)

a) A twin-turbine system was proposed in (Jayashankar et al., 2009; Mala et al., 2011). This configuration develops the rectification concept with the use of a couple of turbines, instead of control valves, as backflow preventers.

Recently, a third possibility has emerged due to its promising results:

b) A new concept of turbine equipped with rectifying valve, presented in (Falcão et al., 2015). The original idea using rectifying valves is reconsidered by means of a sliding-valve in combination with a finger-manifold to drive the flow. The preliminary results are encouraging but the performance of this valve has yet to be tested in tough conditions.

Evidently, the lack of moving parts and valves in the second option makes this possibility the most attractive in terms of maintenance costs.

The twin-turbine system is based on the use of two turbines, one of them working normally (direct mode-outflow) while the other is working as a backflow preventer (reverse mode inflow). A sketch of this system is shown in Figure 1. Basically, the air from the chamber is pushed towards the atmosphere in an exhalation process, so the flow generated passes through the turbines. One of the turbines is working normally, in direct mode (producing energy), whereas the other is working in reverse mode (not producing energy). Once the exhalation process is over, inhalation starts. The air is sucked from the atmosphere to the chamber with the result that the turbines alternate their roles. Note that the flow rate distribution between the turbines, which are working under the same pressure difference (chamber-ambient), is determined by the performance curve of the turbine, which is different for both modes.

The twin system permits the use of unidirectional turbines, which are more efficient than self-rectifying ones. In fact, all the proposals found in the open literature are considering axial turbines (Takao and Setoguchi, 2012) although it has been shown (Pereiras et al., 2014) that flow leakage through the turbine working in reverse mode is around 30% of the total flow generated by the OWC. This important loss of energy hinders the total efficiency of the system, due not only to the flow rate through the turbine which is not producing energy, but also to the braking torque exerted on that turbine (Pereiras et al., 2014).

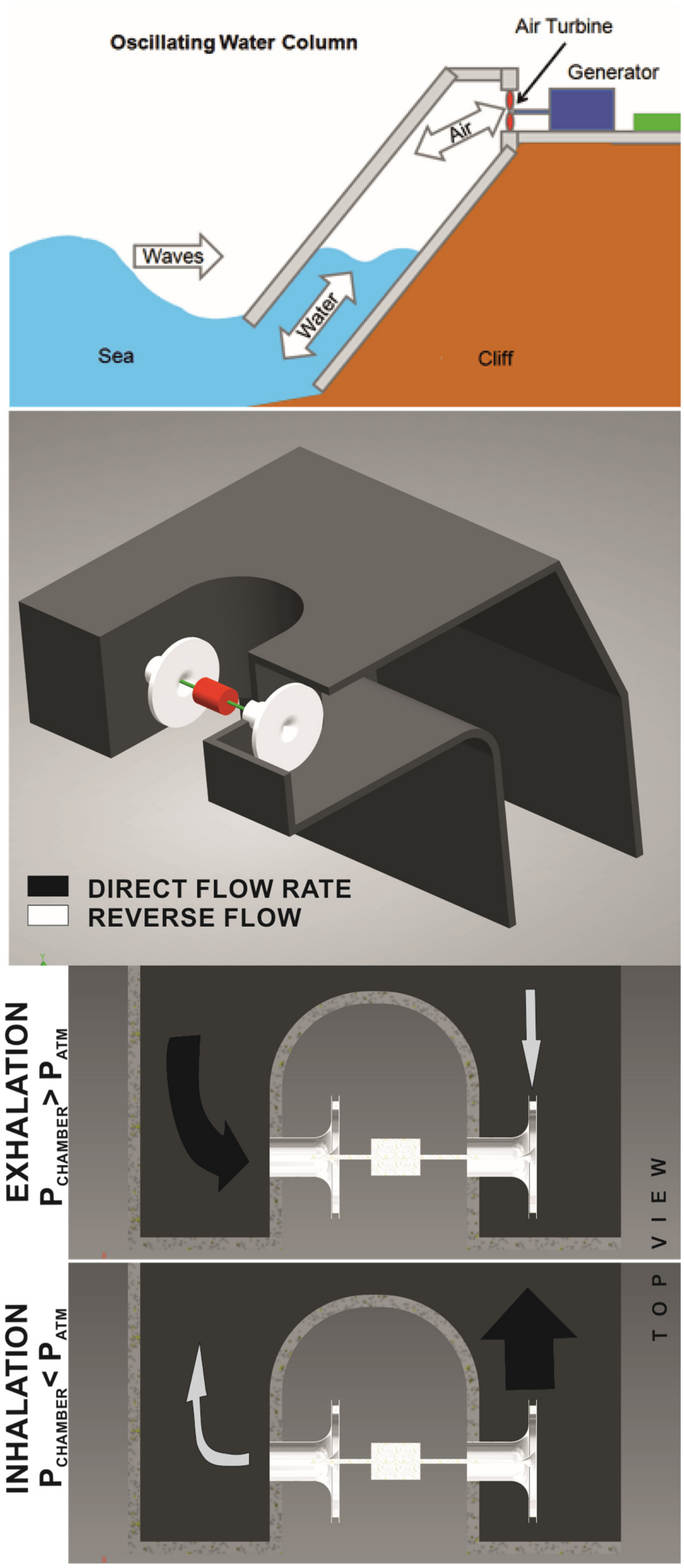

Figure 1. Top: OWC sketch; Middle: OWC equipped with twin radial turbines; bottom: flow distribution.

A fluidic diode is discussed in (Dudhgaonkar et al., 2011) as a possible solution to minimize the reversed flow increasing flow blockage, although results combining the diode with the twin turbines are not presented.

In the present work, a comparison of the performance of radial turbines with respect to axial turbines for twin-turbine configurations is presented. Previous studies of self-rectifying turbines (Pereiras et al., 2011b) reveal that radial turbines show an interesting feature for the twin turbine system: the greater pressure drop generated predicts a significant improvement when operated as backflow preventers, thus providing a minimum energy loss through the turbine working in reverse mode. To the best of the author's knowledge, this is the first time that radial turbines have been proposed for use on twin systems for OWC converters.

The performance curve of the radial turbine is required for a comparison to be made with the axial turbine. For this purpose, a centrifugal turbine has been designed and its performance has been assessed by means of a CFD simulation using the commercial code ANSYS Fluent®. The model has been validated, and shows a good degree of congruence with the experimental results obtained in a test campaign. The performance of the turbine working in both direct and reverse modes has been evaluated, with special attention being paid to that obtained in reverse mode, which was key when selecting a centrifugal turbine instead of a centripetal one. Finally, a numerical estimation of the performance of the whole twin system has been carried out.

The following sections describe in detail the twin-system concept with radial turbines. First of all, in section two, this brand new design is presented to the readers with sound arguments that justify this particular choice. Next, details of the construction and testing of an experimental model are given. Subsequently, the numerical model is fully described. The results are shown in section three, starting with the CFD model validation by means of the turbine performance curves. Later, a more thorough analysis of the flow pattern is conducted to find the strong and/or weak points of the design chosen. Finally, some conclusions are presented in section four.

2. EXPERIMENTAL TESTS AND NUMERICAL MODEL

In this section the authors describe the main points related to the experimental tests carried out and the characteristics of the numerical model used in the CFD simulations.

The turbine for the study has been designed as a centrifugal (direct mode) rather than centripetal (reverse mode) rotor, in order to reinforce its performance as a backflow preventer. Previous studies of radial turbines for OWC (Pereiras et al., 2011a, 2011b) reveal that, even in a turbine equipped with guide vanes, a strong swirling appears in the elbow during centripetal performance when performing off of the best efficiency. It should be noted that, unlike traditional centripetal turbines, the flow rate across OWC turbines is highly variable, with a very large operational range and, as a consequence, the flow angle at the rotor outlet is also continuously changing over time between a wide range of values. This inherent characteristic in the performance of OWC turbines led the authors to consider the use of a radial turbine as a perfect candidate in twin turbine configurations, taking advantage of this feature to optimize the reverse mode.

In line with the idea of reinforcing the reverse mode, and in spite of reducing the efficiency in direct mode, the turbine is composed of a single blade row, so there are no guide vanes upstream or downstream of the rotor. The inner guide vanes have been suppressed in order to maximize the swirl generated in centripetal performance (reverse mode). On the other hand, their suppression generates a large incidence loss at the rotor inlet during centrifugal performance (direct mode), which is minimized by adjusting the inner angle of the blade. Including outer guide vanes downstream of the rotor in centrifugal performance to work as a diffuser would increase maximum efficiency in direct mode. However, it is also known that, off of the best efficiency point, outer fixed guide vanes are an important source of incidence loss in centrifugal performance (Pereiras et al., 2011b). Moreover, the presence of outer guide vanes would facilitate the flow to enter the rotor centripetally (reverse mode), which it is completely undesirable if the flow blockage is to be strengthened. As a result, outer guide vanes were not included in the design.

In the absence of guide vanes, blade design was conducted by means of one-dimensional theory for turbomachines (Dixon and Hall, 2005). Several blade profiles were analyzed by 2-D simulations with the ANSYS Fluent® code. Finally, a 3-D numerical model of the turbine was developed with the selected blade profile. It is appropriate to underline that the design is focused on strengthening blockage in reverse mode, even if that means a reduction of efficiency in direct mode, because this can make the difference with respect to axial turbines for twin systems.

2.1. Experimental tests

A full 3-D turbine prototype was built, according to the scheme shown in Figure 2, in a 3-D printer: BQ Witbox, with a maximum capacity of 297x210x200 mm^3 and maximum resolution of 50 μm. The rotor (Figure 2, top), made of Acrylonitrile Butadiene Styrene (ABS), is shrouded by a ring glued at the tip of the blades in order to reduce the tip flow effect. The connection of the rotor to the two-piece axial tube and the outer diffuser of the turbine was also made in the 3-D printer using Polylactic Acid (PLA) instead. All the components are supported by a central axis (Figure 2, bottom), made of aluminum in a CNC machine. The use of PLA for printing complex pieces in such experimental facilities is highly recommended due to its high degree of finish and ruggedness. Alternatively, ABS can also be used to print out, but it is strongly recommended to use a 3-D printer with a heated plate.

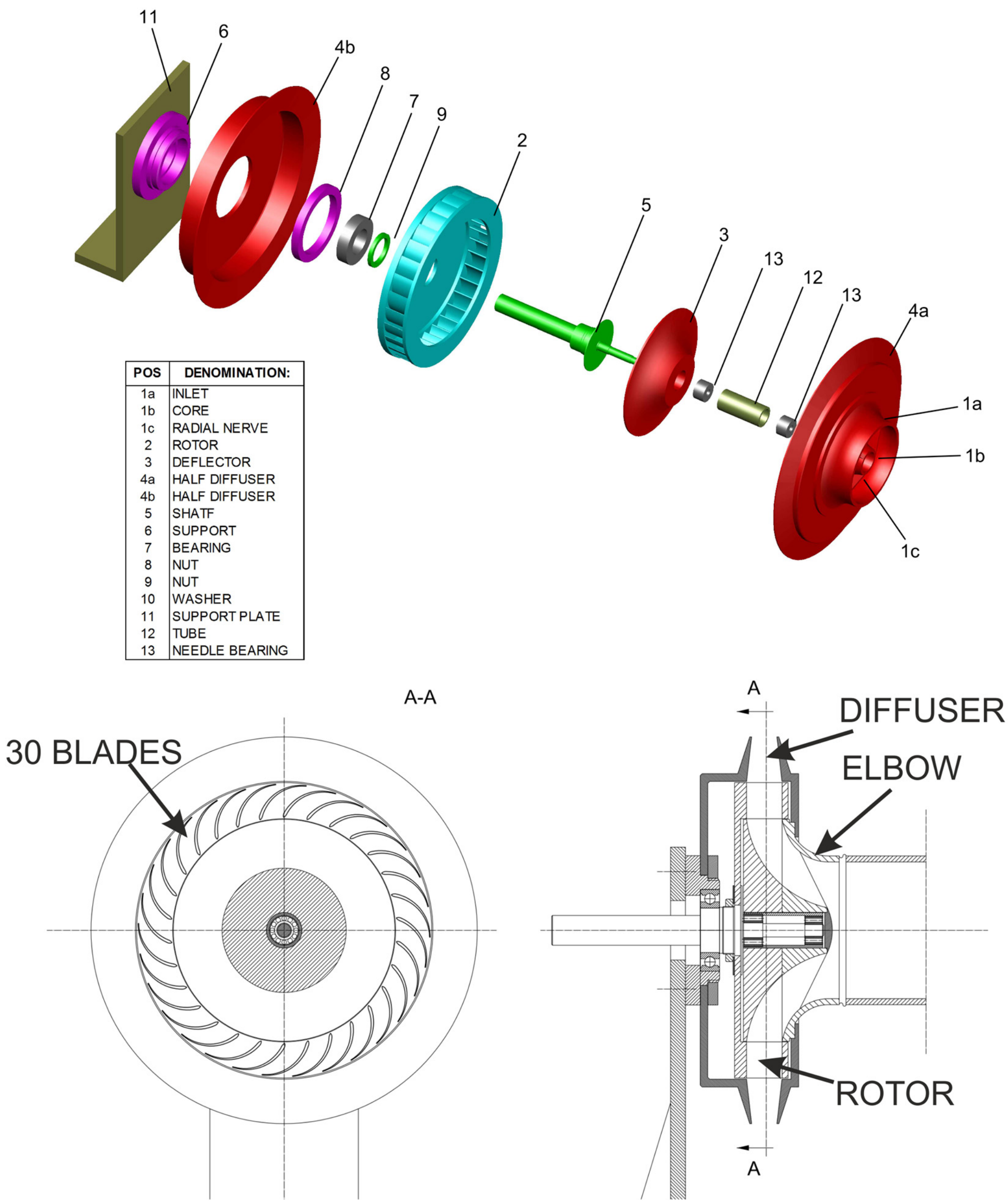

Figure 2. Turbine model

The inner and outer diameters of the radial turbine are 150 and 258.4 mm respectively, with a 24.4 mm span for the blades. The turbine is composed of 30 blades, with inner and outer blade angles of 135 and 175 degrees with respect to tangential direction (i.e. a deflection of 40 deg).

The turbine is mounted in a test rig, as is shown in Figure 3. Flow is generated by a centrifugal fan of 0.75 kW (Soler&Palau CBT-100N). Flow rate was measured with a Venturi-meter with pressure taps connected to a differential manometer.

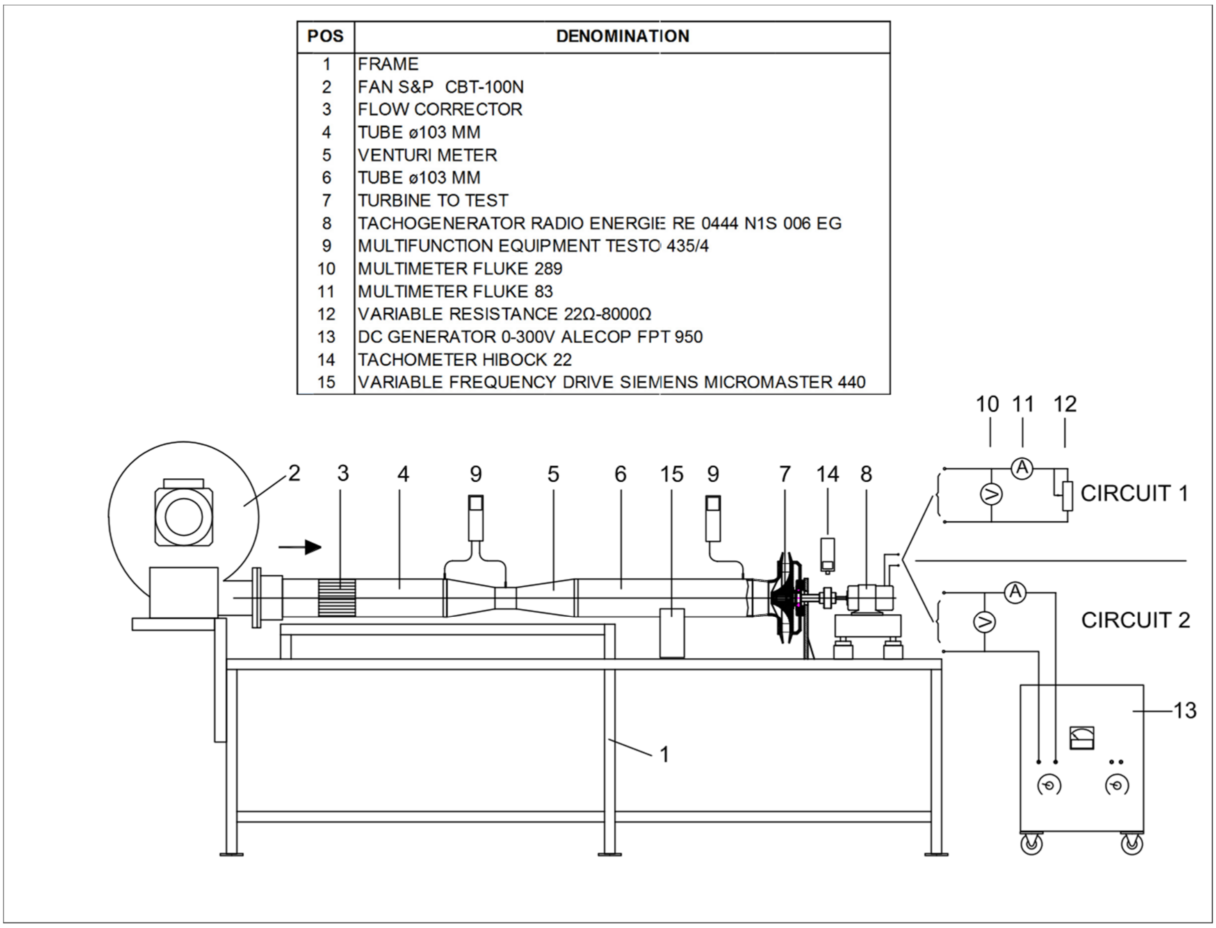

Figure 3. Experimental rig

Information regarding the measuring equipment is shown in Table 1.

Table 1. Information on the instruments used in the experimental tests.

ACCURACY OF MEASUREMENT EQUIPMENT		
Magnitude	**Measurement equipment**	**Minimum accuracy**
Barometric pressure	Station DAVIS VANTAGE VUE 6351	±1 hPa
Room temperature	Testo 435/4	±0,3 ºC
Relative humidity	Testo 435/4	±2 %
Static pressure inlet turbine	Testo 435/4	±2 Pa
Differential pressure in Venturi tube	Testo 435/4	±2 Pa
Angular velocity	Tachometer Hibok 22	±0,15 rpm
Voltage DC	Multimeter Fluke 83	±(0,1%+0,1) V
Intensity DC	Multimeter Fluke 289	±(0,15%+0,02) mA
Resistance DC	Multimeter Fluke 83	±(0,4%+0,1) Ω
Tachogenerator terminal voltage	Tachogenerator RE 0444 N1S 006 EG	±1 %

Turbine input power is determined by the flow rate measured through the venturi tube and the pressure difference between the turbine inlet and the atmosphere.

Assessment of output power was performed by a tachogenerator (Precilec Radio Energie - RE 0444 N1S 006 EG), as follows:

- First of all, electrical loss was assessed according to the data given by the manufacturer, applying the classical theory of electric machines. Next, in order to find a correlation between input power and rotation speed, the tachogenerator was tested alone in motor mode at different constant speeds and unloaded. By discounting previously assessed electrical loss from the measured input power, the mechanical loss of the tachogenerator is found.
- The second step was to assess turbine mechanical loss. Therefore, the turbine was coupled to the tachogenerator to carry out tests at different constant speeds with the tachogenerator running in motor mode. Both total electrical and mechanical tachogenerator loss was discounted from electrical input power, by which mechanical turbine loss was obtained. From these tests a correlation was established between turbine mechanical loss and rotation speed.
- Final tests were carried out to determine turbine output power. The turbine, decoupled from the generator, was installed in the experimental rig, where the fan, conducted by a variable frequency drive, can supply different flow rates. The unloaded turbine is allowed to rotate freely until reaching steady rotation speed, the value of which depends on the flow rate. Since the rotation speed is constant, the torque exerted by the flow is equal to turbine mechanical loss, which can be assessed by the relation between loss and rotation speed from the previous tests.

2.2. Numerical model

Flow simulation is solved with FLUENT v12®, which employs the finite volume numerical method (FVM) to solve the Navier-Stokes equations by using a segregated solver. In order to reduce computational costs, simulations were carried out in a periodic domain (Figure 4). The mesh consists of $2{\cdot}10^6$ hexaedrical cells, with special refinements towards the blade surfaces, and was built in GAMBIT® 2.4.

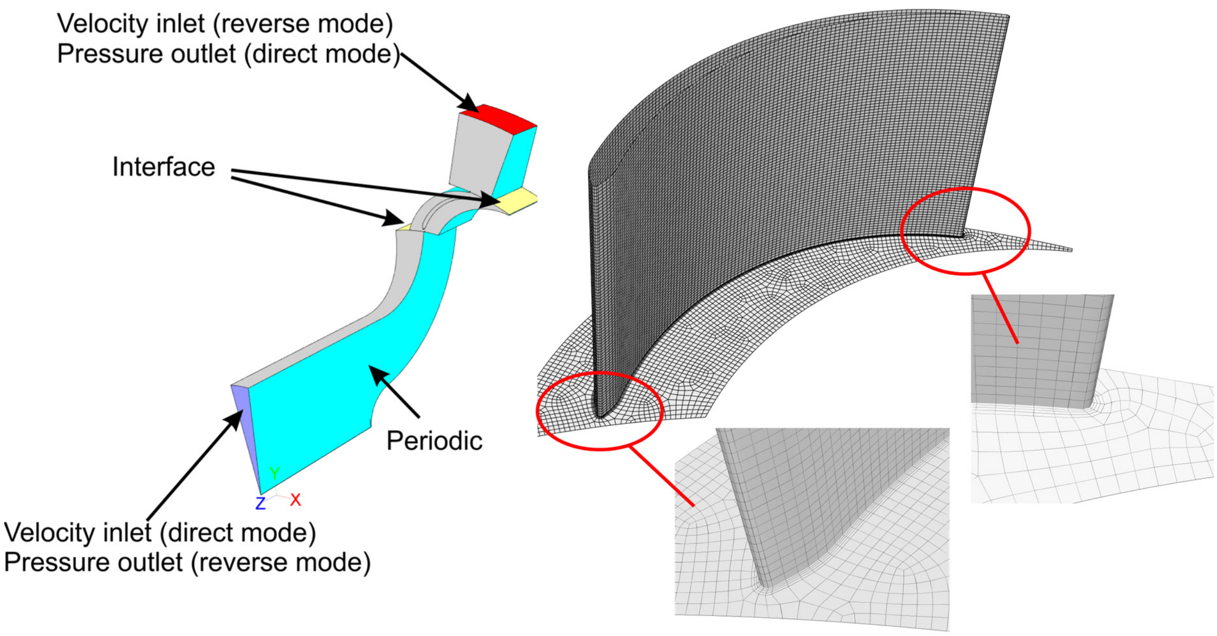

Figure 4. Left: Numerical geometry and boundary conditions. Right: Mesh details

Density was assumed to be constant (1.2 kg/m^3). Once the simulations were over, it was checked that Mach number was below 0.3 in the whole domain.

Since the computational geometry includes rotating domains (ω = 500 rpm), the sliding mesh technique (SMM) was used to control the relative motion of the rotor in a purely unsteady fashion. Therefore, two interfaces were placed upstream and downstream of the rotor (Figure 4). Although SMM was not needed due to the lack of guide vanes, it was in fact used because the model was simulated in batch with other geometries which had guide vanes included.

The realizable *k-ε* turbulence model, already validated in previous works (Pereiras et al., 2011a; Thakker and Dhanasekaran, 2005), was used for the turbulent closure of the numerical model. In addition, a Non-equilibrium Wall Function approach was adopted, so special care was employed in the walls to obtain y^+ values in the corrected range. The time-dependent term is approximated with a second-order implicit scheme. The pressure-velocity coupling was recreated through the SIMPLE algorithm. The high order Monotone Upwind Scheme for Conservation Laws (MUSCL) was used for convection term discretization and the classical central difference approximation for diffusion terms.

The time step was set to 10^{-4} s, resulting in 40 time steps per blade passing period. The residuals were set to 10^{-5} and convergence was achieved after approximately 20 iterations per time step for all the resolved equations. Six full-annulus rotations of the periodical domain were simulated to reach global convergence, with approximately 4 hours of CPU time per flow rate. The simulations were made in a cluster of 4 units with the following characteristics: intel i5 2.67GHz, 2x2 GB RAM.

The simulations were performed on the assumption that the turbine rotated unsteadily but under quasi-steady flow conditions. This assumption is perfectly justified on account of the reduced frequency of the turbine (the ratio between the blade passing period and the period of the wave cycle) which turns out to be 10^3. Therefore, the boundary conditions (flow rate and rotational speed) remain constant in each simulation, although the numerical model is resolved unsteadily since the relative position of the rotor varies with time. The performance of the turbine for other through-flow conditions is obtained by adjusting the flow rate, with the modification of the inlet boundary condition.

3. RESULTS AND DISCUSSION

3.1. Validation and general performance

The usual non-dimensional coefficients are represented below to show the performance of the radial turbine. Specifically, the power and input coefficients, C_P and C_H, as well as the flow coefficient ϕ, together with aerodynamic efficiency, are defined as:

$$C_P = \frac{T_o\,\omega}{\rho\,\omega^3 D^5}\ ,\ C_H = \frac{\Delta P}{\rho\,\omega^2 D^2}\ \ ,\ \phi = \frac{Q/A_R}{u_R}\ ,\ \eta = \frac{T_o\,\omega}{\Delta P\,Q}. \tag{1}$$

Here, ρ is the air density, T_o the mechanical torque, ΔP the total to static pressure difference, Q the flow rate, r_R the blade mid-chord radius, $D=2\cdot r_R$, A_R the cross-flow area at r_R and u_R is the blade speed at r_R. Efficiency, which is the ratio of shaft power output to pneumatic power input, can be expressed in terms of the coefficients mentioned above.

Taking into account the data from Table 1, and following the classical formulation for uncertainty analysis, combined maximum uncertainty is 18% for the input coefficient, 5% for the flow coefficient and 8% for the power coefficient. These values are attained for maximum flow rates but are reduced to 2% in the case of low flow rates.

The performance of the turbine under steady flow conditions and for different flow coefficients is shown in Figure 5. Positive flow coefficients correspond to direct mode, while negative values occur for the turbine working in reverse mode. The results of the numerical model in direct mode (ϕ>0) are compared with the experimental tests made to validate the model. In addition, results for an axial turbine (Pereiras et al., 2014) have also been included for comparison. The numerical power coefficient matches perfectly with the experimental results for the whole range of positive flow coefficients. Also, the development of the input coefficient is accurate, with a discrepancy lower than 10% for the highest flow rates only. Note that this difference is below the maximum experimental uncertainty previously mentioned. Finally, numerical efficiency confirms the excellent agreement with the results in the lab tests, validating the numerical model and allowing an in-depth analysis of the CFD flow patterns.

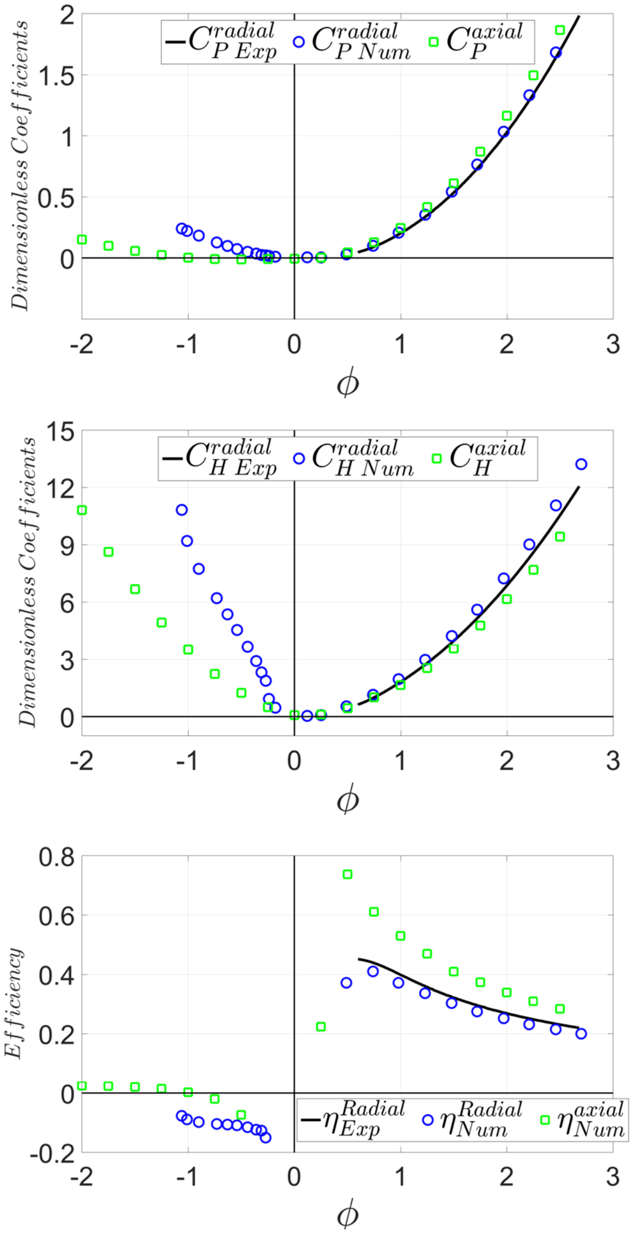

Figure 5. Performance curves of the turbine

Figure 5 (bottom plot) also reveals the main drawback of the radial turbine for this application: its lower efficiency with respect to the axial turbine. In effect, previous studies of axial turbines for OWC report twin systems achieving stationary efficiencies of up to 20% higher (Pereiras et al., 2014; Takao and Setoguchi, 2012). However, the radial turbine would become competitive due to the extreme difference in the input coefficient between direct and reverse modes. The axial turbine (Figure 5 - top plot) exhibits a quite symmetrical distribution of the C_H for both positive and negative flow coefficients, whereas the radial turbine is more likely to impede the reverse flow because of its higher slope in the C_H for negative flow rates. This will be translated into a marginal loss of kinetic energy through the radial turbine, much lower than in the case of the axial turbine, with the result that the radial turbine will perform better as a backflow preventer than the latter (more information on this is provided below).

In addition, it must be appreciated that the braking torque for the reverse mode of the turbine is undesirable, and this negative torque is greater in the radial turbine. However, because of the superior performance of the radial turbine as a backflow preventer, both flow rate and torque will be much smaller than those produced in the axial turbine.

3.2. Flow pattern

In this section, the flow patterns in the radial turbine are analysed in terms of pressure loss and change of momentum (flow angles) in the rotor. The reference angles and velocity relationships are shown in Figure 6 for both direct (centrifugal) and reverse (centripetal) modes.

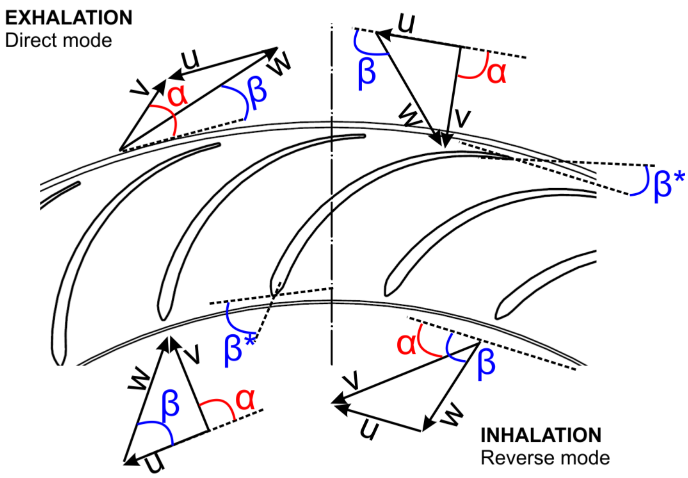

Figure 6. Reference angles and velocity relationships for both direct and reverse modes.

where α and β represent the angles of absolute and relative flow velocities with respect to the tangential coordinate, and β^* is the geometrical blade angle.

To complete the analysis of system losses, the turbine geometry has been divided into three different parts: elbow, rotor and diffuser, Figure 7. Kinetic energy has also been taken into account because of its importance, as is clearly shown in forthcoming figures.

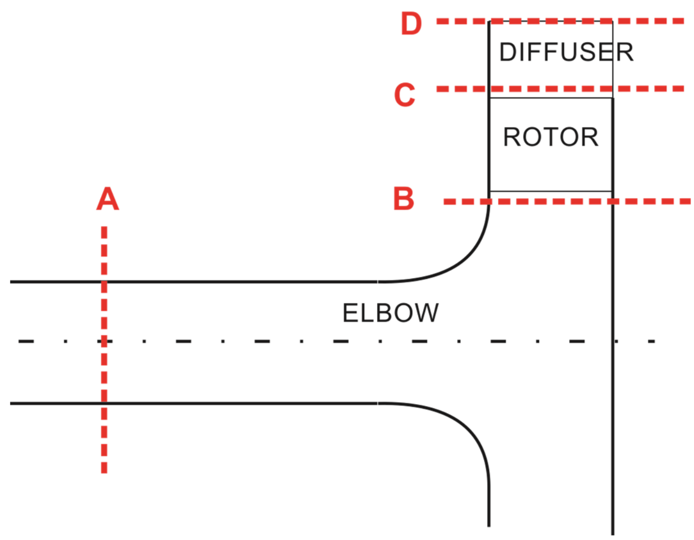

Figure 7. Turbine partition for loss analysis.

Note that energy loss is calculated as the total-to-total pressure difference in terms of every element, taking as references the divisions shown in Figure 7. Hence, dynamic pressure at the outlet (*A* in reverse mode, and *D* in direct mode) is considered as kinetic energy loss.

The loss distribution among the different elements of the turbine are shown in Figure 8 for direct mode. Here, the contributions of the elbow, rotor, external diffuser (as identified in Figure 2) and kinetic energy loss at the outlet are addressed separately. It is clear that the rotor accounts for the greater part of the loss for low-flow coefficients, which is mainly the result of the incidence of the flow. The difference between the flow and blade angles at the inlet is shown in Figure 9, revealing large incidence losses at the blade leading edge, which leads to a critical drop in efficiency when ϕ<1. Also, it can be observed that the entire turbine has its top efficiency point around ϕ =0.7, which does not exactly correspond to the maximum point of efficiency of the rotor (though not shown here, it is found to be around ϕ =1). This fact reveals that the diffuser has a critical role in the machine's efficiency, especially at large flow coefficients. In addition, Figure 8 illustrates how kinetic energy loss at the outlet increases sharply with the flow rate, following a typical parabolic development.

The rise in kinetic energy loss at the outlet is related not only to the flow rate, but is also conditioned by the high values of tangential velocity at the rotor outlet. Figure 10 indicates that the absolute flow angle is abruptly reduced for flow coefficients higher than 0.3, which leads to a strong tangential component and extremely high values of kinetic energies at the outlet. Consequently, this residual kinetic energy is the main source of loss at a high flow coefficient, and is even more important than incidence losses at the rotor (they are reduced for large flow coefficients - Figure 9). Furthermore, the contribution of loss in the diffuser is only important for flow rates below ϕ =0.5 (its relative significance being practically constant for the whole range of large flow rates), while losses at the elbow are practically negligible.

In summary, kinetic energy at the outlet is a critical factor that penalizes the efficiency of the radial turbine in direct mode. Future designs of radial turbines for OWC converters must take particular care with this residual energy to increase efficiencies.

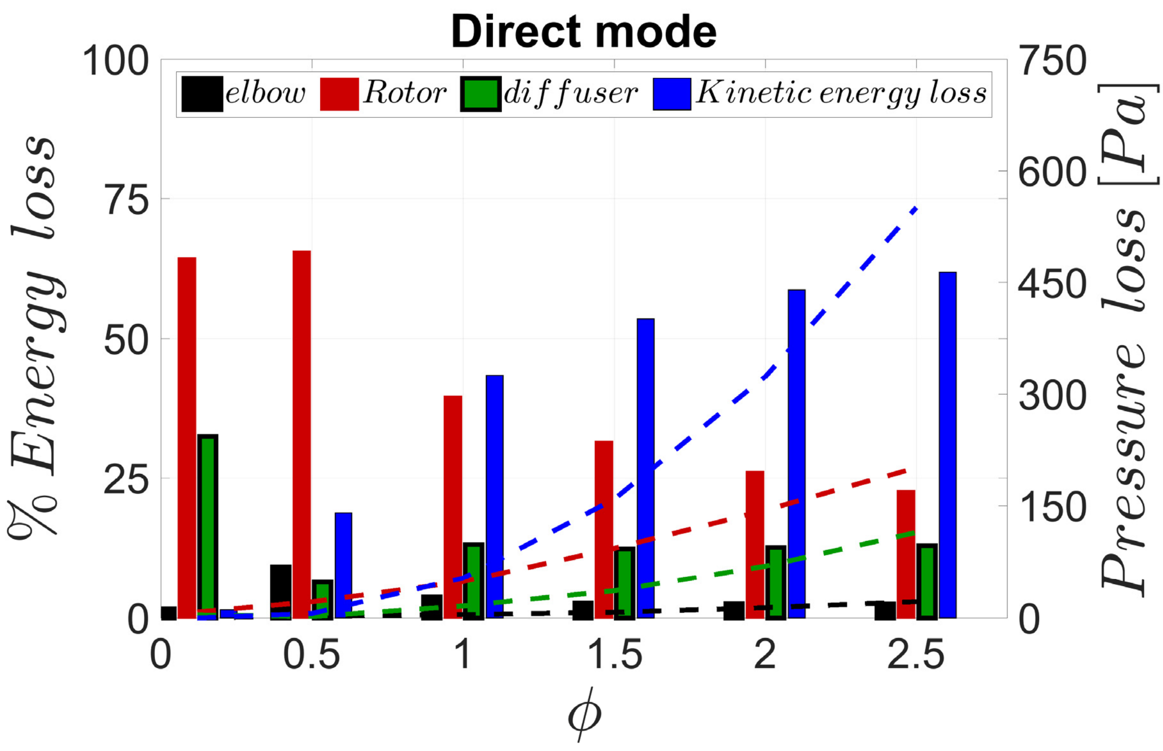

Figure 8. Loss distribution in direct mode. Left axis: Bars, percentage value; Right axis: lines, absolute value.

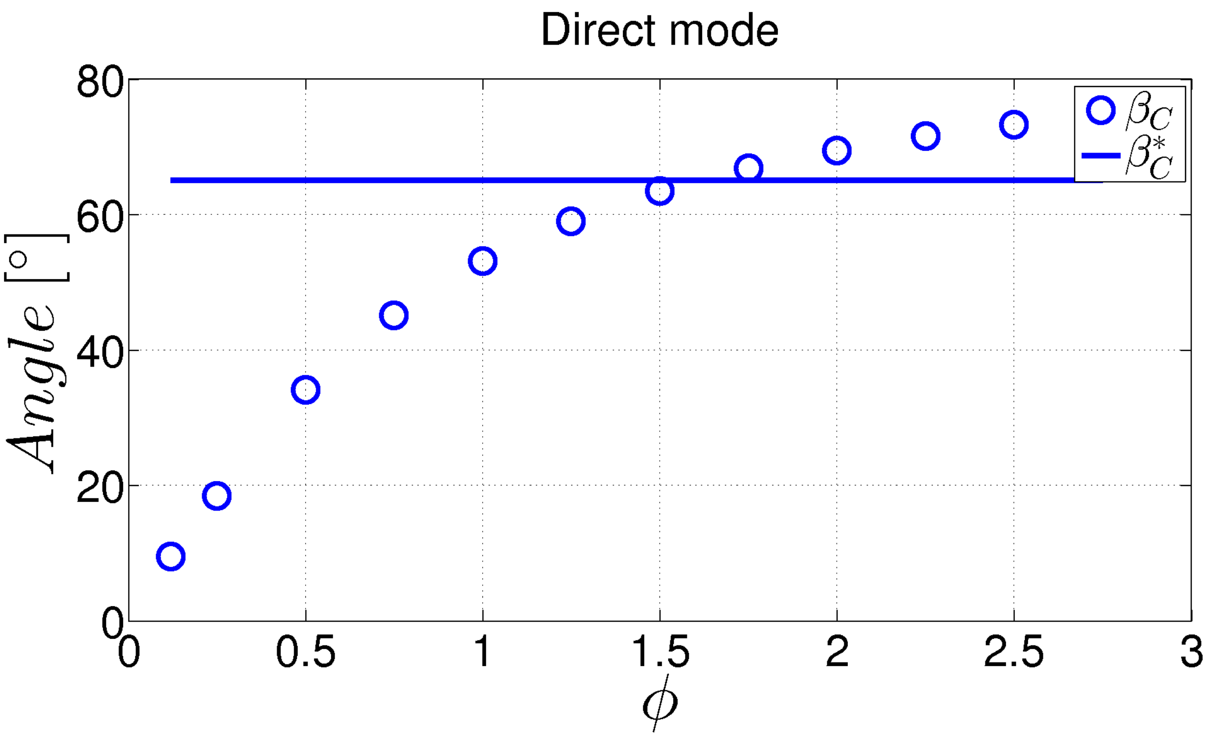

Figure 9. Relative flow angle at the rotor inlet in direct mode.

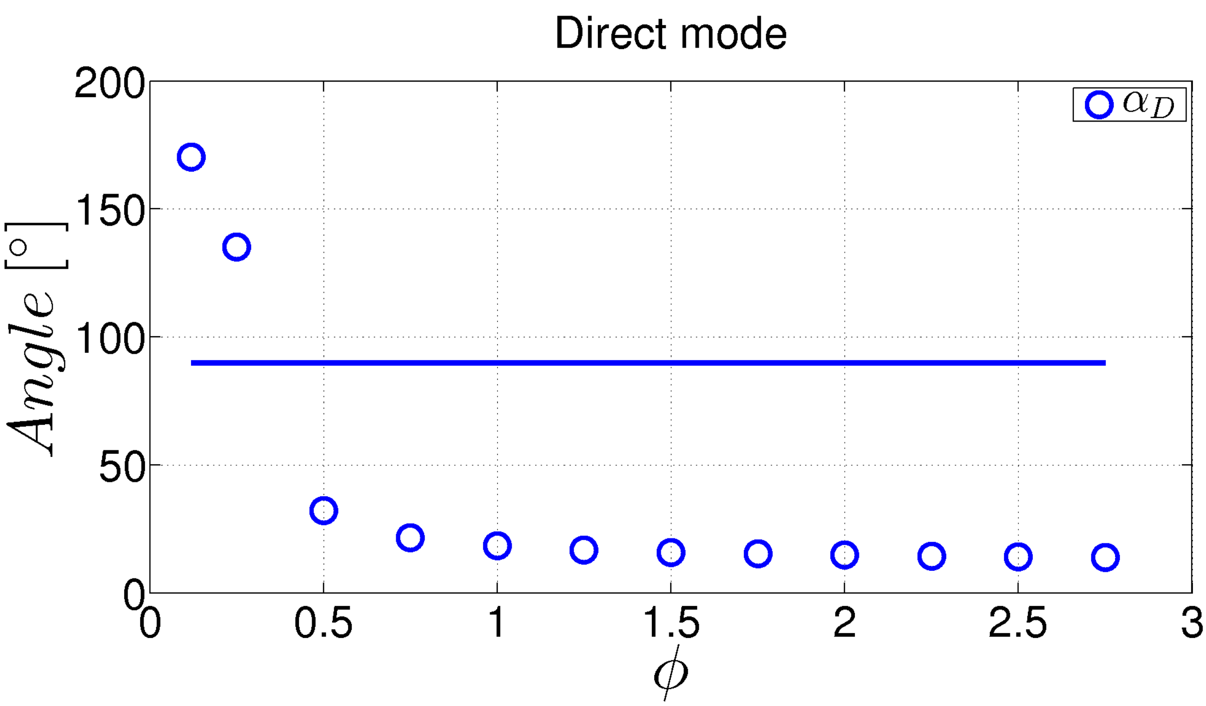

Figure 10. Absolute flow angle at the rotor outlet in direct mode.

Loss distribution is shown for reverse mode in Figure 11. In this case, air flows through the turbine in the centripetal direction, emanating from the diffuser and passing through the rotor and elbow to discharge into the inner duct.

Figure 11 is probably the most important figure in this study, because it shows why this kind of turbine might deserve further analysis. Unlike axial turbines for twin systems, where losses are mainly concentrated in the rotor due to the large incidence flow angles (Pereiras et al., 2014), the main source of loss in the radial version is the elbow. The rotor also displays significant losses (approximately 25% for all the flow rates in Figure 11), on account of the large incidence angle at the inlet in reverse mode (Figure 12). However, as the flow leaves the rotor with a large tangential velocity (see Figure 13), a strong swirling effect takes place and a large amount of loss is generated at the elbow. The large flow blockage caused by the elbow in this centripetal mode demonstrates the appropriateness of employing a radial turbine with a centrifugal direct mode, instead of a traditional centripetal Francis turbine. Moreover, as a result of the large outlet section, both energy losses at the outlet are negligible. Similarly, losses at the diffuser are negligible because, in reverse mode, the incoming flow direction is centripetal.

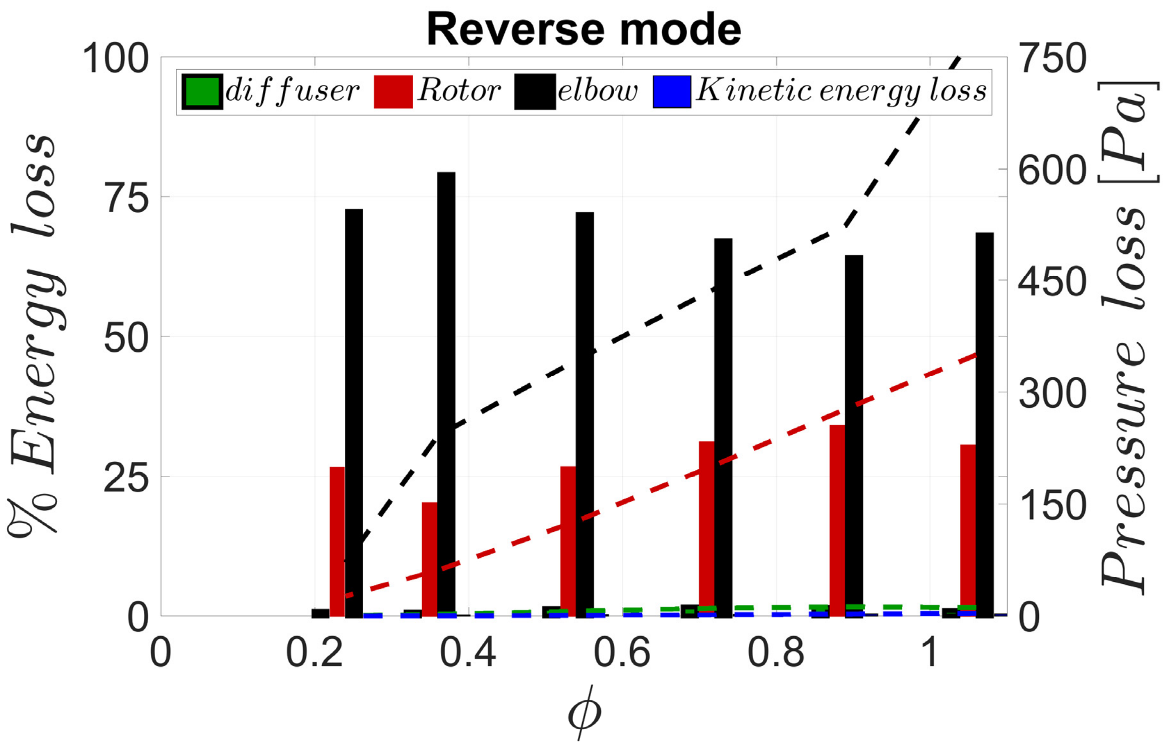

Figure 11. Loss distribution in reverse mode. Left axis: Bars, percentage value; Right axis: lines, absolute value.

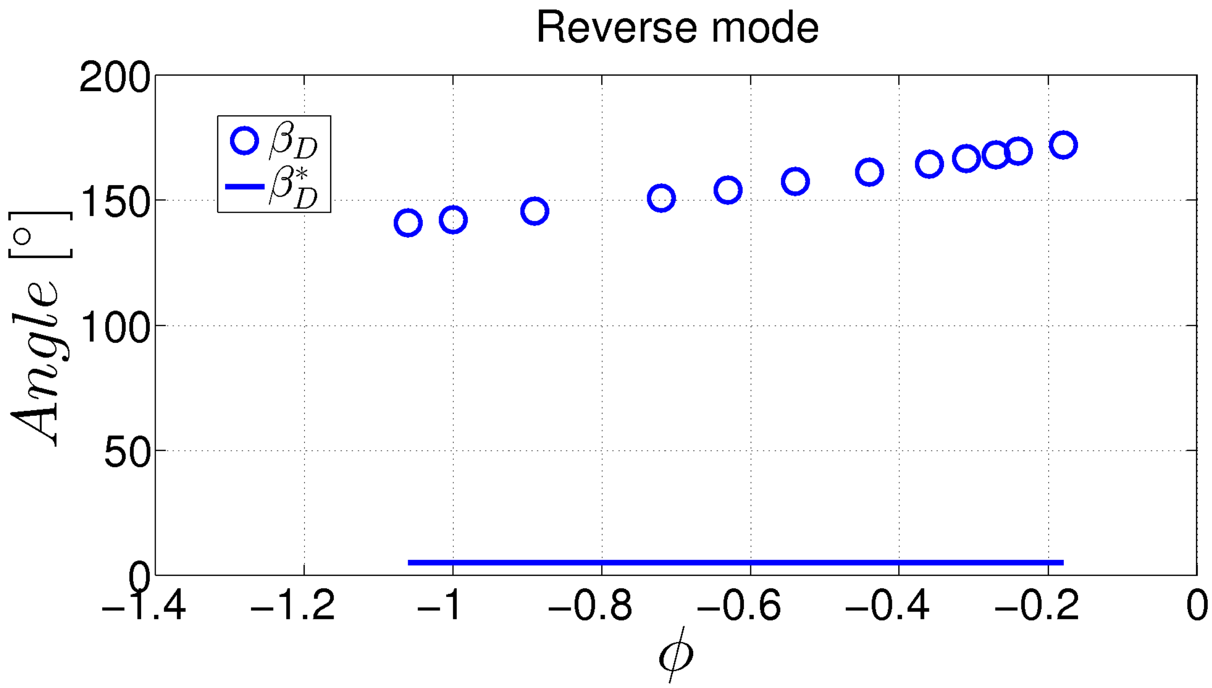

Figure 12. Relative flow angle at the rotor inlet in reverse mode

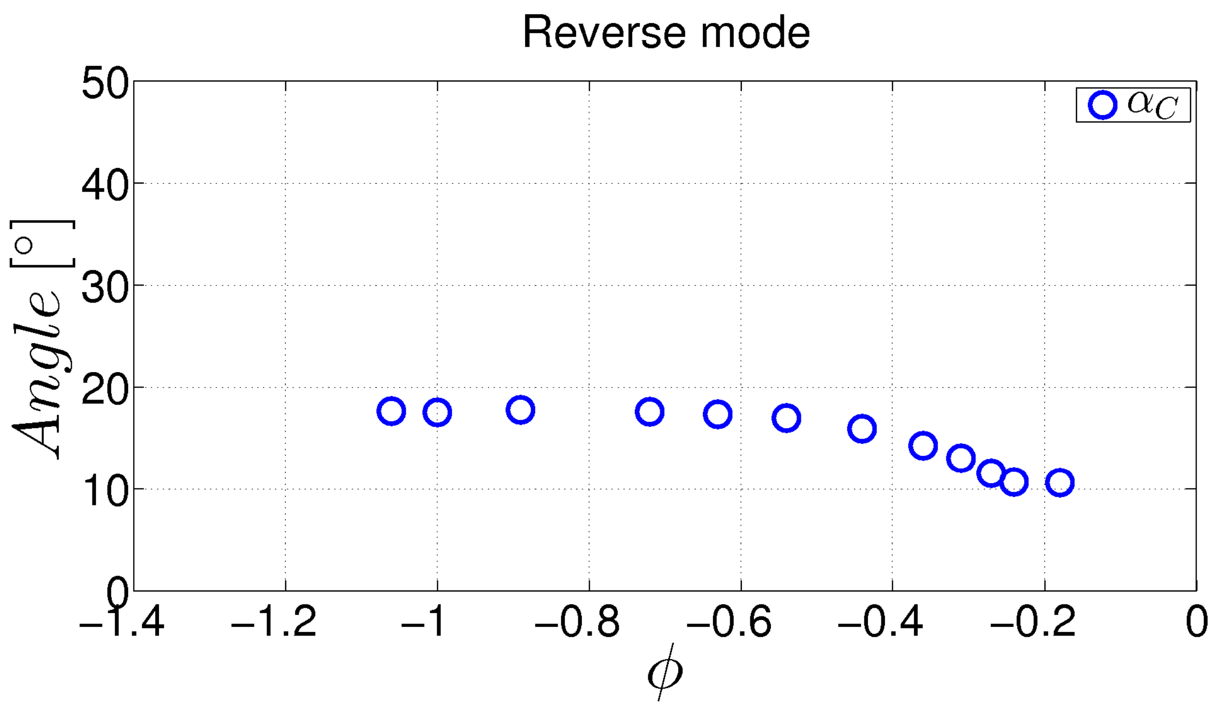

Figure 13. Absolute flow angle at the rotor outlet in reverse mode

3.3. Non-steady performance

Once the analysis of the flow pattern inside the turbine has been completed, it is necessary to evaluate the performance of the whole system in non-stationary conditions. This is achieved by coupling overall turbine performance (the curves shown in Figure 5) with the behaviour of the OWC converter. For this purpose, it has been assumed that the flow rate generated by the OWC device is a sinusoidal function of time (Pereiras et al., 2014; Takao et al., 2011), according to which:

$$Q_{total} = Q_{max} \sin(2\,\pi\,t\,/T) \tag{2}$$

$$\omega \quad = \omega_1 = \omega_2 \tag{3}$$

$$Q_{total} = q_{direct} + q_{reverse} \tag{4}$$

$$\Delta P \quad = \Delta P_1 = \Delta P_2 \tag{5}$$

$$\Phi = (Q_{max}/A_R)/u_R \tag{6}$$

Here Q_{total}, Q_{max}, t and T represent the total flow rate throughout the whole system, the amplitude of the Q_{total}, time and the period of the OWC motion; q is the flow rate through a turbine and subscripts *direct* and *reverse* denote the performance mode of the turbine; ω and ΔP are the rotation velocity and drop in pressure, both being equal for the two turbines of the twin turbines system. Φ represents the dimension-less form of the flow coefficient amplitude for the whole system (including both direct and reverse flows).

Note that this non-steady analysis is made using a total-to-static pressure drop between the inlet and outlet sections of the turbine ($P_{total}^{in} - P_{static}^{out}$), rather than the total pressure differences the authors used in previous studies (Pereiras et al., 2014). Therefore, kinetic energy losses at the outlet are taken into account.

The performance of OWC turbines is commonly considered quasi-steady when working on an OWC converter (Inoue et al., 1988; Setoguchi and Takao, 2006; Takao et al., 2011). This reasonable assumption permits a non-steady comparison between turbines based on steady performance data.

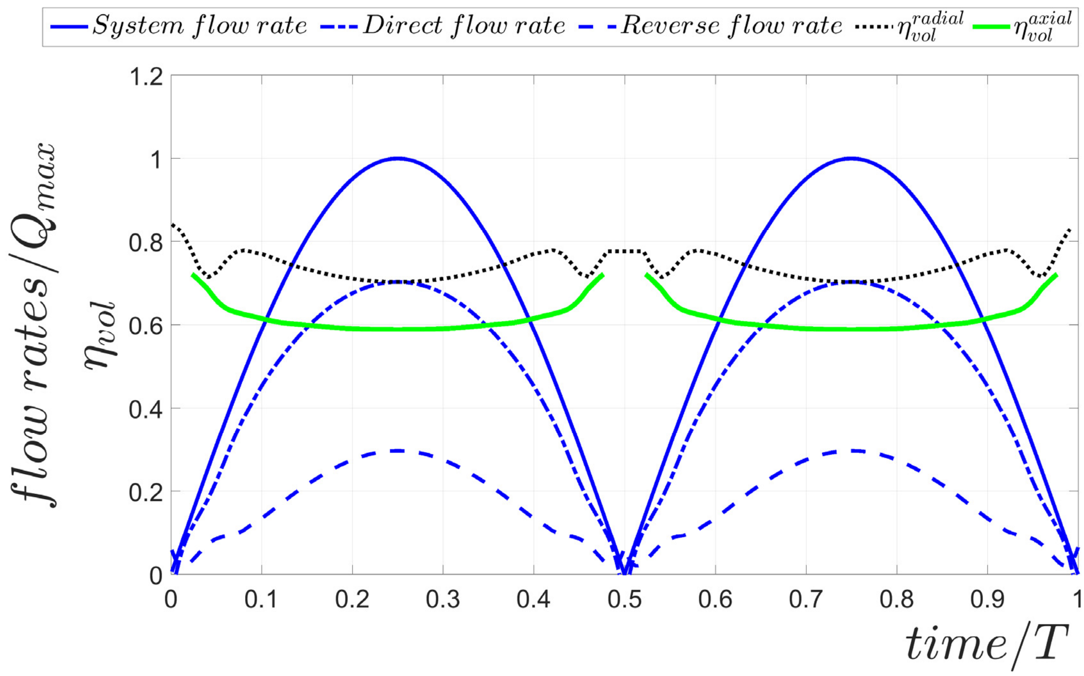

Figure 14. Flow rate distribution under sinusoidal total flow rate ($\Phi = 1.5$).

After the previous resolution of the equation system (2) to (5) using the performance curve of the radial turbines, it is possible to represent the periodic behavior of the flow rate, as well as other variables of interest. In Figure 14, both sinusoidal distributions of the instantaneous flow rate for both turbines in direct and reverse modes are compared with the total flow rate in the chamber. The flow rates are made non-dimensional with the maximum flow rate in the OWC system, Q_{max}, and the time is divided by the wave period. In addition, volumetric efficiency, defined as $\eta_{vol} = q_{direct} / Q_{total}$, is plotted for both axial and radial turbines.

Since the η_{vol}^{radial} is over 70%, less than 30% of the flow generated by the OWC escapes through the turbine working in reverse mode; this is lower than the flow leakage produced in a twin turbine equipped with axial turbines, which reaches values up to 42%. It is important to underline, as was mentioned before, that this leakage is not only untapped energy; note that larger flow rates through turbines in reverse modes imply larger breaking torques (Figure 5).

Evaluation of the system's performance is in terms of the mean efficiency, which is defined as:

$$\overline{\eta}_{system} = \frac{\frac{1}{T}\int_0^T \omega\, T_{total}\, dt}{\frac{1}{T}\int_0^T \Delta P_t\, Q_{total}\, dt} = \underbrace{\frac{\frac{1}{T}\int_0^T \Delta P_t\, q_{direct}\, dt}{\frac{1}{T}\int_0^T \Delta P_t\, Q_{total}\, dt}}_{\overline{\eta}_{input}} \underbrace{\frac{\frac{1}{T}\int_0^T \omega\left(T_{direct}+T_{reverse}\right) dt}{\frac{1}{T}\int_0^T \Delta P_t\, q_{direct}\, dt}}_{\overline{\eta}_{tg}} \tag{7}$$

where T_{total} is the total torque on the electricity generator. Therefore:

$$\bar{\eta}_{system} = \bar{\eta}_{input}\ \bar{\eta}_{tg} \tag{8}$$

Mean input efficiency, η_{input}, is a parameter closely related to the volumetric efficiency of the system (Figure 14), whereas twin-turbines efficiency, η_{tg}, is the efficiency of the twin turbine group, calculated with regard to the flow rate, which is supposed to produce energy (q_{direct}).

There are references (Takao et al., 2011) where the η_{tg} is calculated by not taking into account the torque of the turbine in reverse mode, despite the fact that the flow through the turbine in reverse mode is being considered. This common hypothesis is a reasonable assumption if the turbine running in reverse mode is disconnected from the rotating axis with some disrupting element. In this study, and in order to be conservative, the torque in reverse mode has been preserved in the definition.

Figure 15 shows the different efficiencies for the twin-turbine configuration for both radial and axial turbines. The results show that maximum total efficiency of the system (η_{system}) is 24% in the case of the radial turbine. As expected, the axial turbine (using performance data from (Takao et al., 2011) has a significantly higher value, reaching 34% at Φ =1 (solid green line). If only efficiency of the turbines is considered, the superior performance of the axial machine is demonstrated, with enhancement of η_{tg} by up to 20% in the case of axial turbines. However, the strong feature of the radial turbines is the remarkable η_{input}, close to 80% for the optimal range of flow coefficients (around Φ=1.4). Therefore, the poor efficiency of the radial turbine in direct mode is significantly balanced by a superior performance in reverse flow conditions.

Consequently, radial turbines can be an interesting option for an OWC device with a twin turbine configuration, provided that more developments are carried out with regard to turbine blades; this would increase the efficiency of the turbine itself (with the current design, the difference in η_{tg} is still excessively favorable for axial turbines).

Bridging this gap, the greater volumetric efficiency of the radial turbines, combined with the sharp reduction in flow leaking through the reverse mode turbine, may be key factors to justify the development of a new generation of twin-turbine prototypes with radial architecture.

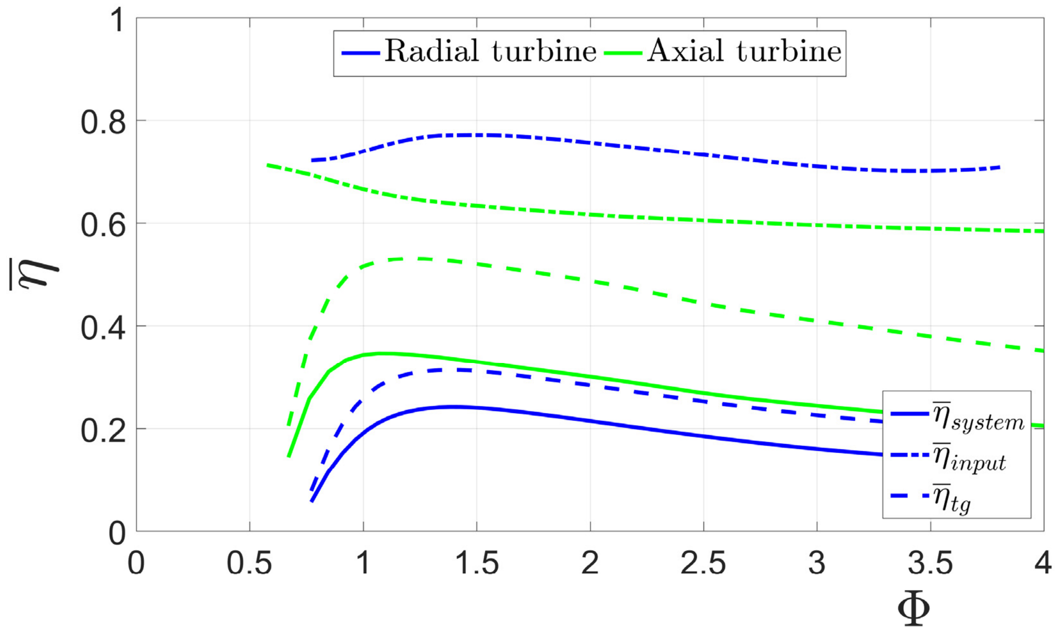

Figure 15. Mean efficiencies of the twin turbine system with radial turbines compared to axial turbines (data taken from (Takao et al., 2011)).

4. CONCLUSIONS

This paper studies the performance of OWC devices, based on a twin turbine configuration, with radial turbines. To the best of the authors' knowledge, the use of a radial turbine to enhance flow rectification in twin turbine systems is presented for the first time in the open literature.

Firstly, a CFD model of the radial turbine has been validated and employed to assess turbine performance in both modes of operation: direct (centrifugal) and reverse (centripetal). It is shown that the large pressure drop generated in reverse mode implies enhanced exploitation of the energy produced by the OWC because only a reduced part of the total flow rate leaks through the turbine working in reverse mode. Despite of the lower efficiencies found in radial turbines, their improved performance as backflow preventers in comparison with axial machines makes radial turbines a promising option for being installed in twin turbines systems.

To be fully competitive, the major challenge is to close the gap in the performance of radial turbines for direct mode. In particular, a greater effort regarding design is needed to reduce the large kinetic energy loss of radial turbines at the outlet. An improvement in the blade profiles, combined with a reduction in flow deflection, could reduce this detrimental effect and improve efficiency in direct mode. Alternatively, performance in reverse mode could be preserved, because the main amount of loss, namely, the swirl at the elbow, is not dependent on the blade’s external angle.

In summary, although much work is still required to improve the performance of radial turbines in centrifugal operation, this research demonstrates that radial turbines can be a suitable option for use in twin turbine configurations for OWC power plants.

5. ACKNOWLEDGEMENTS

The authors acknowledge the support provided by "Centro Integrado de F.P. Mantenimiento y Servicios a la Producción de Langreo", with special mention to its Director, Mr. F. Fanjul.

6. REFERENCES

Babintsev, I.A., 1975. Apparatus for converting sea wave energy into electrical energy. Patent nº US 3922739.

Curran, R.; Denniss, Tom; Boake, C., 2000. Multidisciplinary design for performance ocean wave energy conversion, in: Proceedings of the 10th International Offshore Polar Engineering Conference. Seatle.

Dixon, S.L., Hall, C.A., 2005. Fluid mechanics and thermodynamics of turbomachinery, 5th ed. Elsevier Butterworth–Heinemann, Oxford.

Dudhgaonkar, P. V., Jayashankar, V., Jalihal, P., Kedarnath, S., Setoguchi, T., Takao, M., Nagata, S., Toyota, K., 2011. Fluidic components for oscillating water column based wave energy plants, in: ASME-JSME-KSME 2011 Joint Fluids Engineering Conference: Volume 1, Symposia – Parts A, B, C, and D. ASME, Hamamatsu, Japan, pp. 1979–1983. doi:10.1115/AJK2011-07035

Falcão, A.F. de O., 2010. Wave energy utilization: A review of the technologies. Renew. Sustain. Energy Rev. 14, 899–918. doi:10.1016/j.rser.2009.11.003

Falcão, A.F.O., Gato, L.M.C., 2012. Air Turbines, in: Sayigh, A.A. (Ed.), Comprehensive Renewable Energy. Elsevier, Oxford, pp. 111–149. doi:10.1016/B978-0-08-087872-0.00805-2

Falcão, A.F.O., Gato, L.M.C., Henriques, J.C.C., Borges, J.E., Pereiras, B., Castro, F., 2015. A novel twin-rotor radial-inflow air turbine for oscillating-water-column wave energy converters. Energy 93, 2116–2125. doi:10.1016/j.energy.2015.10.046

Falcão, A.F.O., Henriques, J.C.C., 2016. Oscillating-water-column wave energy converters and air turbines: A review. Renew. Energy 85, 1391–1424. doi:10.1016/j.renene.2015.07.086

Inoue, M., Kaneko, K., Setoguchi, T., Saruwatari, T., 1988. Studies on the Wells turbine for wave power generation (turbine characteristics and design parameter for irregular wave). JSME Int. J. 31, 676–682. doi:10.1299/jsmeb1988.31.4_676

Jayashankar, V., Anand, S., Geetha, T., Santhakumar, S., Jagadeesh Kumar, V., Ravindran, M., Setoguchi, T., Takao, M., Toyota, K., Nagata, S., 2009. A twin unidirectional impulse turbine topology for OWC based wave energy plants. Renew. Energy 34, 692–698. doi:10.1016/j.renene.2008.05.028

Maeda, H., Santhakumar, S., Setoguchi, T., Takao, M., Kinoue, Y., Kaneko, K., 1999. Performance of an impulse turbine with fixed guide vanes for wave power conversion. Renew. Energy 17, 533–547. doi:10.1016/S0960-1481(98)00771-X

Maeda, H., Takao, M., Setoguchi, T., Kaneko, K., Kim, T.H., 2001. Impulse turbine for wave power conversion with air flow rectification system, in: Proceedings of the 11th International Offshore and Polar Engineering Conference. Stavanger, Norway.

Mala, K., Jayaraj, J., Jayashankar, V., Muruganandam, T.M., Santhakumar, S., Ravindran, M., Takao, M., Setoguchi, T., Toyota, K., Nagata, S., 2011. A twin unidirectional impulse turbine topology for OWC based wave energy plants - Experimental validation and scaling. Renew. Energy 36, 307–314. doi:10.1016/j.renene.2010.06.043

Pereiras, B., Castro, F., el Marjani, A., Rodríguez, M. a., 2011a. Tip clearance effect on the flow pattern of a radial impulse turbine for wave energy conversion. J. Turbomach. 133, 41019. doi:10.1115/1.4002409

Pereiras, B., Castro, F., Marjani, A. el, Rodríguez, M.A., 2011b. An improved radial impulse turbine for OWC. Renew. Energy 36, 1477–1484. doi:10.1016/j.renene.2010.10.013

Pereiras, B., Valdez, P., Castro, F., 2014. Numerical analysis of a unidirectional axial turbine for twin turbine configuration. Appl. Ocean Res. 47, 1–8. doi:10.1016/j.apor.2014.03.003

Raghunathan, S., 1995. The Wells air turbine for wave energy conversion. Prog. Aerosp. Sci. 31, 335–386. doi:10.1016/0376-0421(95)00001-F

Setoguchi, T., Santhakumar, S., Takao, M., Kim, T.H., Kaneko, K., 2002. A performance study of a radial turbine for wave energy conversion. Proc. Inst. Mech. Eng. Part A J. Power Energy 216, 15–22. doi:10.1243/095765002760024917

Setoguchi, T., Takao, M., 2006. Current status of self rectifying air turbines for wave energy conversion. Energy Convers. Manag. 47, 2382–2396. doi:10.1016/j.enconman.2005.11.013

Takao, M., Setoguchi, T., 2012. Air turbines for wave energy conversion. Int. J. Rotating Mach. 2012. doi:10.1155/2012/717398

Takao, M., Takami, A., Okuhara, S., Setoguchi, T., 2011. A twin unidirectional impulse turbine for wave energy conversion. J. Therm. Sci. 20, 394–397. doi:10.1007/s11630-011-0486-1

Thakker, A., Dhanasekaran, T.S., 2005. Computed effect of guide vane shape on performance of impulse turbine for wave energy conversion. Int. J. Energy Res. 29, 1245–1260. doi:10.1002/er.1117

Torre-Enciso, Y., Ortubia, I., López de Aguileta, L.I., Marqués, J., 2009. Mutriku wave power plant: from the thinking out to the reality, in: 8th European Wave and Tidal Energy Conference (EWTEC 2009). Uppsala, Sweden, pp. 319–328.

Wells, A.A., 1980. Rotary transducers. Patent nº US4221538 A.